Three-dimensional holographic lithography by an iterative algorithm

Joshua J. Cowling,[1,]* Gavin L. Williams,[2] Alan Purvis,[1] Richard McWilliam,[1] Jose J. Toriz-Garcia,[2] Nicholas L. Seed,[2] Florian B. Soulard,[1] and Peter A. Ivey[3]

[1]*School of Engineering and Computing Sciences, Durham University, Durham DH1 3LE, UK*

[2]*Department of Electronic and Electrical Engineering, University of Sheffield, Sheffield S1 3JD, UK*

[3]*Innotec Ltd., P. O. Box 2141, Calver, Hope Valley S32 3YZ, UK*

Corresponding author: j.j.cowling@durham.ac.uk

Received March 16, 2011; revised May 19, 2011; accepted May 31, 2011;
posted June 1, 2011 (Doc. ID 144363); published June 23, 2011

We have applied an iterative algorithm for hologram design with multiple output image planes arranged in close proximity to create continuous patterns within an imaging volume. These holograms have been designed for photolithography on three-dimensional surfaces. The influence of simulated image plane separation on the final image, and its suitability for lithography, is assessed. Results are presented and the most suitable case is demonstrated experimentally. © 2011 Optical Society of America

OCIS codes: 090.1760, 110.6895, 230.6120, 110.3960.

Standard lithographic procedures, such as proximity and projection exposure, do not work well for nonplanar substrates. Any conventional two-dimensional (2D) imaging system is limited by the depth of its point-spread function. The image will become distorted away from its flat focal plane, leading to variation in feature width or to insufficient contrast for a well-defined photoresist exposure.

Unlike a standard photomask, holograms can generate three-dimensional (3D) images from 2D representations with relative ease. Computer-generated holograms (CGH) have been used to create focused patterns on 3D substrates [1,2]. This is, however, limited to sparse line patterns. For more complex or dense patterns, mask implementation can become a problem as simultaneous modulation of amplitude and phase may be required.

Optimization procedures based on the Gerchberg–Saxton (GS) algorithm [3] allow for a more general pattern geometry to be generated while maintaining a phase-only CGH. This allows the use of active phase spatial light modulators (SLM) or fixed phase masks for implementation. Holograms generated in this way, however, will tend to produce large noise components in the reconstructed image, resulting in poor photoresist exposures. Others have overcome this by time averaging [4] or by applying more complex systems and modeling techniques [5]. We have found that an iterative algorithm based on the angular-spectrum (AS) transformation can converge to holograms for images containing "thin" (of the order of the width of the point-spread function) binary structures. These are suitable for patterning of integrated circuit interconnections in a lithographic exposure. These methods are usually applied to a single planar image. To extend this to 3D surfaces, we have implemented a multiplane modification similar to [6–8], with further constraints. Specifically: exclusive use of the AS method for propagation to ensure valid patterns over short propagation distances, maintaining a constant sum of squared amplitude values when correcting the hologram in order to help maintain the stability of the iteration, and defining a set of constraints that can result in a useful exposure pattern. We have implemented holograms using a phase-only SLM (pixel pitch 8 μm, active area 1024×1024 pixels).

The algorithm invokes a numerically evaluated AS propagation [9] between uniformly spaced planes inside an image volume and a single diffraction plane (Fig. 1).

The process may be outlined as: (I) a long forward propagation from the hologram to the furthest plane in the image volume; (II) short reverse propagation steps traversing the image volume in conjunction with applying different amplitude constraints across N planes separated by distance δz; (III) a long reverse propagation from the image volume back to the diffraction plane; and (IV) a phase-only constraint applied in the diffraction plane in which it is ensured that the total sum of squared amplitude values remains constant. In step (IV), filtering and spatial constraints may also be applied. As with the GS algorithm, the above process is repeated, and we expect image error to decrease. Through zero padding and splitting of the longer propagation transforms (steps I, III) into multiple steps, we avoid noise caused by aliasing of the transfer function [10].

Amplitude constraints are applied at each image plane (Fig. 2). To enable the algorithm to converge to a useful solution the image volume must not be overconstrained. Our adopted approach is to constrain only those areas on each plane that are in close proximity to the target

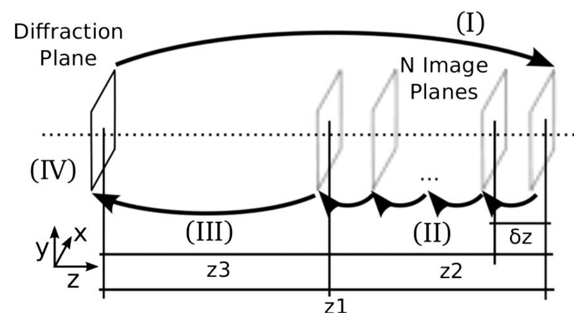

Fig. 1. Multiplane algorithm illustrated. An image volume of depth z_2 is divided into N image planes separated by δz ($\delta_z = z_2/(N-1)$). The image volume is offset from the diffraction plane hologram by z_3.

 © 2011 Optical Society of America

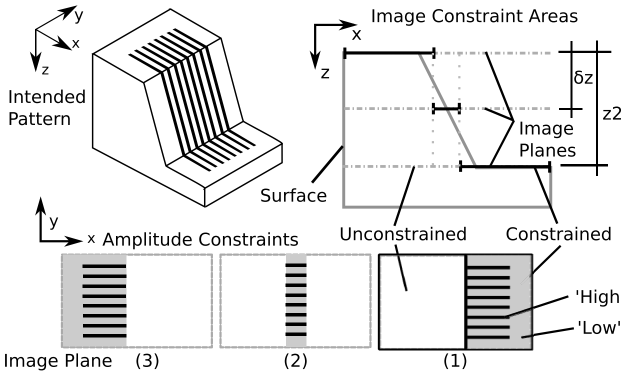

Fig. 2. Multiple plane constraints shown for a sparse case ($N = 3$) Surface patterns are then applied on the nearest constraint plane.

surface. Areas of constraint are applied to mutually exclusive sections of each image plane, so that no constrained area occludes another in the z direction. This kind of constraint pattern has been shown to produce image zones on two planes [7]; however, we apply dense constraints to a real surface and show experimentally that a continuous pattern can be generated onto photoresist. Within the constraint process, "high" regions are given field amplitude value 1 and "low" regions are set to 0.1, while phase is unchanged. Unconstrained areas remain unaltered. As discussed in [8], low regions cannot be set to zero as this would lead to a loss of phase information between propagation steps. The high/low ratio was chosen so as to enforce as large a contrast as possible without overconstraining the requirements on the image field.

The choice of initial "seeding" hologram can influence the structure of the resulting pattern. A random phase distribution often is used, but we have observed more reliable quality when applying an analytically derived initial hologram. To generate the initial hologram, we superimpose planar line segment holograms [2] and then confine the resulting pattern to a phase-only distribution. This produces a nonideal approximation, which is quickly refined. Mathematically, this approximation takes the form

$$U = \left\{ \sum_{m=1}^{M} \left[\exp\left(\frac{i\pi d^2}{\lambda(z_3 + z_2/2)} \right) \right] \right\} \times \mathrm{rect}\left(\frac{x}{A}, \frac{y}{B} \right), \quad (1)$$

where $d = y - pm - s$ and y is the y direction coordinate of the hologram, p is the pitch of the lines to be imaged, s is an offset for alignment, M is the number of lines, and U is the hologram pattern. λ is the wavelength of the illumination source. The 2D rect function limits the size of the hologram according to A and B, where these are determined by the length of the lines and the width of the hologram, respectively. A further step curtails this to a phase-only pattern.

Coherent resolution can be improved by increasing the numerical aperture (NA) of the focusing optical element ($\delta x \approx \lambda/(2\,\mathrm{NA})$). With any pixelated modulator, this is limited by pixel pitch. After evaluating resolution with a set of simulated continuous phase zone plates for the dimensions and pixel pitch of the SLM, we chose to work in a regime away from these pixelation effects at 16 cm where the point size full width at half-maximum (FWHM) measurement is also approximately 8 μm. Analyzing this focal point image along the optical axis and again taking a FWHM measurement, we estimate the depth of focus (DOF) of the system to be 0.92 mm.

A fixed electron-beam written phase mask could improve resolution by using smaller pixels. This will, however, decrease the DOF of a given image point ($\mathrm{DOF} \approx 2\lambda/(\mathrm{NA}^2)$, therefore $\mathrm{DOF} \approx 8\delta x^2/\lambda$), resulting in larger N (smaller δz) required to attain a useful hologram. Furthermore, a fixed mask is likely to restrict the number of quantized phase levels.

Iterative simulations were run at sample pitch 4 μm. An image and hologram size of 8.192 mm × 8.192 mm was chosen. The image comprised eight lines that descend a 45° slope over a total depth of $z_2 = 4.096$ mm (Fig. 2). This represents an image volume that is more than 4 times deeper than the DOF. The lines have a width of 8 μm at a pitch of 24 μm. The image volume is located $z_3 = 16$ cm from the diffractive screen.

A set of holograms was generated, each by performing 50 iterations. Variable N (and subsequently δz) were investigated to determine the minimum number of image planes required.

Simulated image profiles and cross sections can be seen in Fig. 3. Dips in the x profiles occur at the edge of each constrained region and are due to a combination of out-of-focus image patterns as the sloped surface is descended, and interference between the patterns imposed on separate planes. Images generated were assessed according to the contrast parameter $C = (H - L)/(H + L)$ [11] shown in Fig. 4. We set L to the maximum background noise intensity value (i.e., in the "low" constrained regions, calculated from profiles taken between the image lines) and H to the minimum intensity value along simulated profiles of the lines (i.e., along the "high" constrained regions). This stringent measurement is calculated over the intended 3D focal surface for an upsampled hologram at increased resolution after the

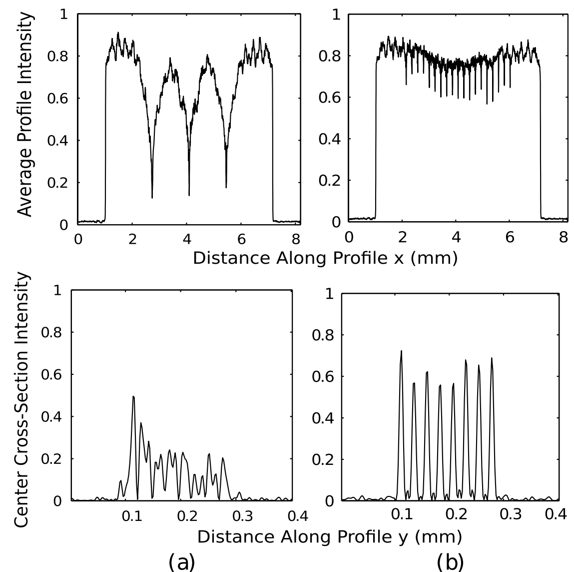

Fig. 3. Example average intensity profiles and center cross sections for simulated nonplanar surface. (a) $N = 4$ ($\delta z = 1365\,\mu$m), (b) $N = 20$ ($\delta z = 215\,\mu$m).

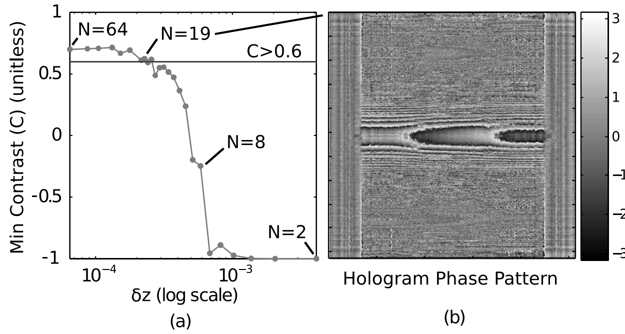

Fig. 4. (a) Simulated contrast for variable plane separation (δz plotted on a log scale). (b) Hologram for $N = 19$. Analog phase pattern shown. Resampled for implementation. Size is 1024×1024 pixels at $8\,\mu$m pitch.

iterative procedure. This provides a comparison of pattern continuity, since higher contrast will result in a better-defined exposed image area.

Minor fluctuations present in the contrast graph [Fig. 4(a)] demonstrate sensitivity to local defects generated by the iterative process. If we choose contrast $C > 0.6$ as an approximate limit for lithography [11], then this strict "worst-case" metric shows that for our simulations at $\delta z \approx 228\,\mu$m ($N = 19$) and below, a consistent and useful image can be generated. This value equates to $\delta z \approx 0.25 \times$ DOF for this system. Test exposures were performed to confirm continuous patterns in the focal region. The hologram generated for $N = 19$ was used [Fig. 4(b)], as this is close to the lowest viable computing effort. In implementation on our SLM, we used all of the 256 phase levels available. This exhibits little difference from the nonquantized pattern in simulation. This number of quantized phase levels could be significantly reduced without compromising contrast greatly. We have observed useful output with as few as eight phase levels. The optical setup is shown in Fig. 5.

The hologram was implemented on an $8\,\mu$m sample pitch SLM (Pluto, Holoeye Photonics AG) by quantizing and resampling the phase pattern. This device is illuminated by an on-axis expanded laser beam (Coherent Cube 405 nm 50 mW). The photoresist used was BPRS200 from Fuji Photo Film Co. Ltd. This layer was approximately $2\,\mu$m thick. Images of the pattern developed on a glass substrate are shown in Fig. 6. Lines of requisite shape can be seen on both flat and tilted sections with only small line width variation noticeable at the edges of constraint areas on separate planes.

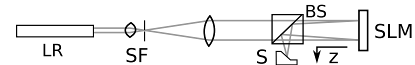

Fig. 5. Exposure setup. Laser (LR), spatial filter/beam expansion (SF), beam splitter (BS), modulator (SLM), substrate (S).

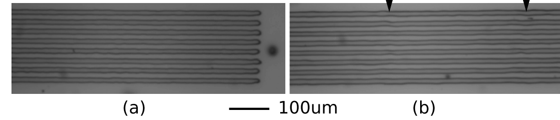

Fig. 6. Photoresist pattern on (a) flat-top surface, (b) 45° sloped surface. Hologram used was $N = 19$ ($\delta z = 228\,\mu$m). Arrows indicate areas at the edge of image constraints for separate planes.

In conclusion, we have shown that simple phase-only holograms generated by an iterative method can be used to produce continuous patterns of dense lines suitable for microelectronics fabrication on grossly nonplanar substrates. We have demonstrated this method by patterning an example where eight lines of pitch $24\,\mu$m have a final developed track width $\approx 9.6\,\mu$m. These have been patterned onto a slope that is more than four times deeper than the DOF of the optical system. The example presented is well beyond a conventional 2D projection system with a similar resolution limit.

References

1. J. J. Toriz-Garcia, G. L. Williams, R. McWilliam, R. Curry, N. L. Seed, A. Purvis, and P. A. Ivey, J. Micromech. Microeng. **20**, 015012 (2010).
2. A. Maiden, R. McWilliam, A. Purvis, S. Johnson, G. L. Williams, N. L. Seed, and P. A. Ivey, Opt. Lett. **30**, 1300 (2005).
3. R. W. Gerchberg and W. O. Saxton, Optik **35**, 237 (1972).
4. C. Bay, N. Huebner, J. Freeman, and T. Wilkinson, Opt. Lett. **35**, 2230 (2010).
5. S. Bühling, F. Wyrowski, E. Kley, A. Nellissen, L. Wang, and M. Dirkzwager, J. Micromech. Microeng. **11**, 603 (2001).
6. R. Dorche, A. Lohmann, and Sinzinger, Appl. Opt. **33**, 869 (1994).
7. J. Xia and H. Yin, Opt. Eng. **48**, 020502 (2009).
8. M. Makowski, M. Sypek, A. Kolodziejczyk, and G. Mikula, Opt. Eng. **44**, 125805 (2005).
9. J. Goodman, *Introduction to Fourier Optics*, 3rd ed. (Roberts and Company, 2005).
10. M. Sypek, J. Opt. Commun. **116**, 43 (1995).
11. A. Wong, *Resolution Enhancement Techniques in Optical Lithography* (SPIE Press, 2001).